Surg Today (2011) 41:733–736
DOI 10.1007/s00595-010-4316-y

SURGERY TODAY
© Springer 2011

Case Report

Sigmoid Colon Perforation Induced by the Vascular Type of Ehlers–Danlos Syndrome: Report of a Case

HIROSHI OMORI[1], ATSUSHI HATAMOCHI[2], MAKOTO KOIKE[1], YOSHITOSHI SATO[1], TOMOKI KOSHO[3], YASUHITO KITAKADO[1], TAKAFUMI OE[1], TOSHIKI MUKAI[1], YOKO HARI[1], YOSHIFUMI TAKAHASHI[1], and KENJI TAKUBO[1]

[1]Department of Digestive Surgery, Matsue Red Cross Hospital, 200 Horomachi, Matsue, Shimane 693-8501, Japan
[2]Department of Dermatology, Dokkyo Medical University, Mibu, Tochigi, Japan
[3]Department of Medical Genetics, Shinshu University, Matsumoto, Nagano, Japan

Abstract
The vascular type of Ehlers–Danlos syndrome (vEDS) is a rare inherited disease of the connective tissues, and is caused by abnormal type III collagen resulting from heterogeneous mutations of the type III collagen *COL3A1* gene. We herein report the case of a vEDS patient who developed a sigmoid colon perforation and was given a definitive diagnosis by a genetic and biomolecular assay. The patient demonstrated clinical manifestations caused by tissue weakness such as frequent pneumothorax events and a detached retina. During the operation, we noticed easy bruising and thin skin with visible veins on the patient's abdominal wall. Finally, a diagnosis was confirmed by the reduction of type III collagen synthesis and by the identification of a mutation in the gene for type III collagen. We conclude that it is difficult to diagnose a vEDS patient without clinical experiences and specialized genetic methods. Furthermore, all organs must be treated gently during therapy, because the tissues of vEDS patients are extremely fragile.

Key words Ehlers–Danlos syndrome · Vascular type · Perforation · Type III collagen · *COL3A1*

Introduction

The vascular type of Ehlers–Danlos syndrome (vEDS, Ehlers–Danlos syndrome type IV) is a rare, autosomal dominant disease of the connective tissues caused by abnormal type III collagen resulting from heterogeneous mutations of the type III collagen *COL3A1* gene.[1–4] vEDS is characterized by four clinical criteria: easy bruising, thin skin with visible veins, characteristic facial features, and the rupturing of arteries and organs.[1–4] In addition, classic EDS patients exhibit hypermobility of the large joints and hyperextensibility of the skin.[1,2] Typically, Ehlers–Danlos syndrome (EDS) is divided into six types, and vEDS patients follow a particularly poor clinical course caused by complications from tissue weakness.[1,2] Twenty-five percent of vEDS patients develop one or more complications associated with tissue weakness by 20 years of age, and 80% develop some complications by 40 years. Pepin et al. reported that the calculated median survival time of vEDS patients was 48 years of age.[1] We herein present a case report of a vEDS patient who was clinically and genetically diagnosed following a sigmoid colon perforation, and review the pertinent literature.

Case Report

A 20-year-old male patient was admitted to our hospital with severe abdominal pain. The patient's abdominal wall was very hard, and muscular guarding was palpated. Enhanced computed tomography was performed immediately, and revealed free air and stool containing barium in the abdominal cavity, because the patient's colon had been examined 2 days prior for causal ascites and abdominal pain by a barium enema (Fig. 1A,B). As soon as we diagnosed the patient with generalized peritonitis due to colon perforation, an emergency operation was performed. During the operation, the patient's abdominal skin was observed to be markedly thin, with visible veins. After we decided that the sigmoid colon perforation was the cause of the generalized peritonitis, the lesion was removed and Hartmann's procedure was performed. In addition, it was revealed that the patient suffered from frequent spontaneous pneumothorax events in the past, and that his creatine kinase levels

Reprint requests to: H. Omori
Received: November 15, 2009 / Accepted: February 22, 2010

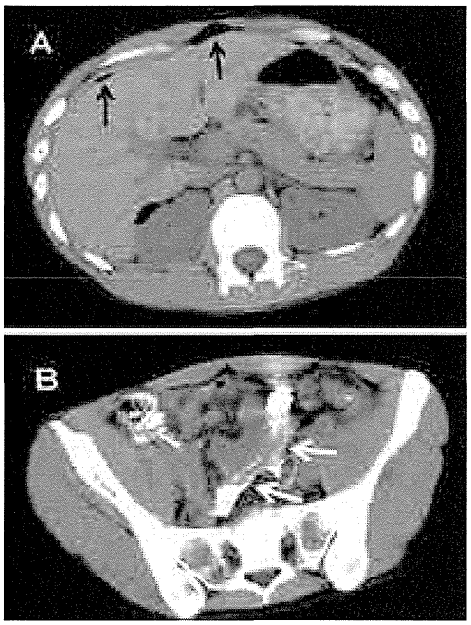

Fig. 1A,B. Enhanced computed tomography at the sigmoid colon perforation. Free air (*black arrows*) and stool containing barium (*white arrows*) were observed in the abdominal cavity

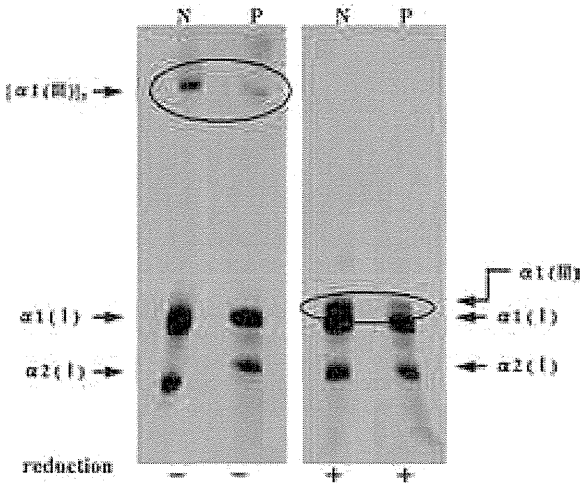

Fig. 2. Production of type I or type III collagen in the patient's cultured fibroblasts. The synthesis of type I collagen in this patient was the same as in controls. However, the synthesis of type III collagen was reduced by approximately 22.7% compared with the normal control values (*inside circle*). *N*, normal control; *P*, patient with vascular type of Ehlers–Danlos syndrome

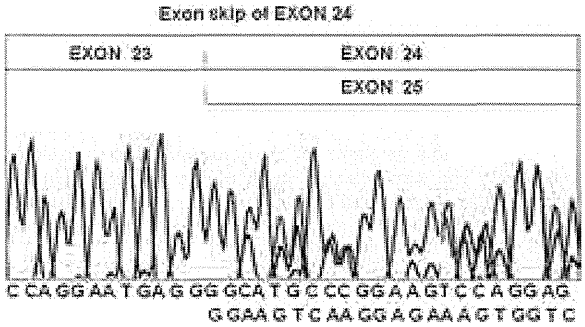

Fig. 3. Genetic analysis of the complementary DNA from the patient's cultured fibroblasts. A skip in exon 24 of *COL3A1*, which encodes collagen type III, was identified by the genetic analyses of the complementary DNA from the cultured fibroblasts

were increased to severalfold higher than in normal subjects. Although a paralytic ileus developed as a complication, the patient was discharged from our hospital 1 month after the operation. However, 3 days after discharge, he was readmitted due to his eighth spontaneous pneumothorax and a detached retina in his left eye. Because many complications caused by tissue weakness had developed over such a short period, very rare vEDS was diagnosed according to the four clinical criteria: easy bruising, thin skin with visible veins, characteristic facial features, and rupture of the arteries and organs.

To confirm this diagnosis, the patient's skin and blood samples were sent to Dokkyo Medical University, and were examined by genetic and molecular biological assays. Accordingly, the diagnosis of vEDS was confirmed by the reduction of type III collagen synthesis in cultured skin fibroblasts and by the identification of a mutation in the gene for type III collagen (*COL3A1*). The synthesis of type I collagen in this patient was the same as in controls. However, the synthesis of type III collagen was reduced by approximately 22.7% compared with normal controls (Fig. 2). A skip in exon 24 of *COL3A1*, which codes for collagen type III, was identified by genetic analysis of the complementary DNA from cultured fibroblasts (Fig. 3). Furthermore, the region near the genomic DNA was amplified by polymerase chain reaction (PCR) for the analyses of genomic DNA; the result revealed a G-to-A transition at the donor splice-site +1 of intron 24 (IVS 24 G+1 to A) of the *COL3A1* gene (Fig. 4). Because the mother of the present patient also demonstrated characteristic facial features and easy bruising of the skin, we genetically examined her blood samples to determine the genetic background of this patient. Consequently, we were able to confirm that the mother had the same mutation in *COL3A1* gene.

Less than 6 months after the sigmoid colon perforation, the patient was admitted with a developing

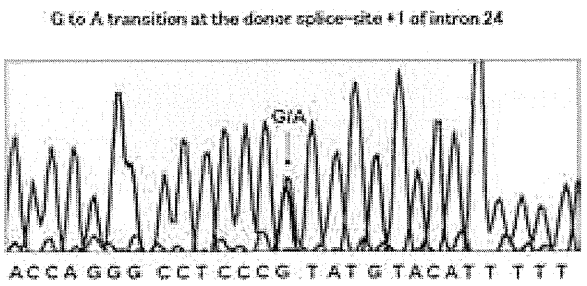

Fig. 4. Sequence analysis of genomic DNA from the patient's blood cells. The region near the genomic DNA was amplified by polymerase chain reaction for the analysis of genomic DNA. The results revealed a G-to-A transition at the donor splice site +1 of intron 24 (IVS 24 G+1 to A) of the *COL3A1* gene

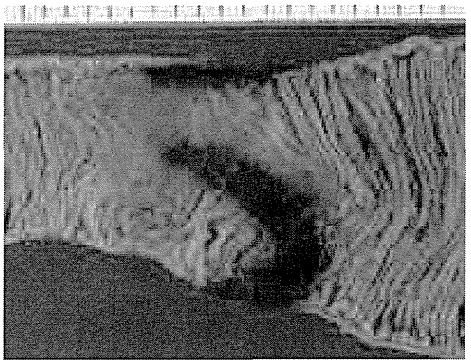

Fig. 5. Resected specimen of the jejunum from the second operation. The seromuscular layer of the patient's jejunum was torn throughout, and the entire layer of the intestine had become partly necrotic

adhesive ileus. Although conservative therapy was appropriated because there was no ischemic change of the intestine at admission, an emergency operation was performed because of the sudden onset of severe abdominal pain, which was not relieved by analgesic drugs. The operative and histopathological findings revealed the seromuscular layer of his jejunum to be torn, thus resulting in partial necrosis of this entire layer of the patient's intestine (Fig. 5). Therefore, we performed a partial resection of the small intestine, and the colostomy was not closed.

Methods of Genetic Examination

Dermal fibroblasts were obtained from the patient's skin and were cultured.[5–7] The protein synthesis of type I and type III collagen were assessed as described previously.[5–8] After RNA was extracted from the cultured fibroblasts, complementary DNA was synthesized by reverse transcription from the RNA as a template. The complementary DNA was amplified by PCR, and analyzed by electrophoresis on polyacrylamide gels to identify the abnormal fragments. Abnormal DNA fragments were directly sequenced by an ABI PRISM 3100 genetic analyzer (ABI Advanced Biotechnologies, Columbia, MD, USA).[2,3,8] Furthermore, genomic DNA was extracted from the blood cells, and all mutations were confirmed in the genomic DNA of *COL3A1* by a sequence analyzer.[2,3,8]

Discussion

Ehlers–Danlos syndrome (EDS) is a rare inherited disease of the connective tissue.[1,2] Most surgeons generally consider EDS to be a dermatologic disease.[1–4] However, patients who are affected by EDS, particularly the vascular EDS type (vEDS), develop complications associated with tissue weakness, and surgical or interventional therapy is often required.[1–4,9–11] Until genetic and biochemical testing was sufficiently developed, a considerable number of patients who died unexpectedly could not be diagnosed as having vEDS. In the present case, the reason for the colonic perforation was unclear after a histopathological examination, and 6 months passed until the diagnosis of vEDS could be made by genetic and biomolecular assays. Even if we suspected the possibility of vEDS based on the patient's clinical symptoms, the genetic and biomolecular assays could not be easily performed in most hospitals. Fortunately, we obtained advice from an authority in genetics and had technical support with the genetic and biomolecular assays. If this patient had not been definitively diagnosed, it is likely that the patient and his family might have lost any hope. Our belief is that a system for diagnosing rare inherited diseases, such as vEDS, should therefore be established as expeditiously as possible in Japan.

In general, most surgeons encounter vEDS patients who are affected by perforative peritonitis and perform surgery by creating an intestinal stoma, because the abdominal cavity is polluted with stool and the patient's tissues are very fragile. Furthermore, the intestinal stoma helps in the management of constipation, which these patients often experience to a severe extent.[1] The existence of an intestinal stoma is also preferable in order to prevent high intestinal pressures. However, patients who receive a colostomy creation are typically frustrated by the limited lifestyle. Therefore, while we understand why a patient may prefer bowel reconstruction, it is difficult to proceed down this path. It is necessary to consider the future of the vEDS patients, as it may be safer not to remove the intestinal stoma to

prevent high intrabowel pressure that causes constipation and adhesive ileus. It is an important to note that complications and tissue weakness increase in vEDS patients after the age of 20 years.[1,2] Several authors have recommended that the perforative lesion and its distal colon should be removed at the same time to prevent reperforation in the sigmoid colon and rectum.[10] Other authors have also recommended a subtotal colectomy as a reasonable treatment because of the high rate of reperforation in vEDS patients.[12] Although these suggestions have validity and are based on a safety-first concept, we were unable to perform a subtotal colectomy for the present vEDS patient at the time of the first operation, when a definitive diagnosis had not yet been determined. Moreover, it is difficult for us to perform both a partial resection of the small intestine and a subtotal colectomy, even at a second operation, because of the risk of short bowel syndrome and anastomotic leakage. It appears that a unique procedure for perforation of the colon in vEDS patients cannot be standardized, because individual patients have widely divergent background factors, such as age, performance status, accuracy of the diagnosis, frequency of perforation, and medical expertise in their country.

We recommend a therapeutic approach for the ileus in vEDS patients based on the clinical course of the present vEDS patient. vEDS patients who are affected by ileus must be surgically treated before too many fissures develop in the intestine, regardless of the presence of ischemic changes. In general, patients who are diagnosed with a paralytic ileus or adhesive ileus after prior operations are conservatively treated by decompression with a nasogastric tube or a Miller–Abbott tube. However, we were unable to treat our vEDS patient conservatively, because the wall of his small intestine was easily torn and became necrotic under high pressure. The timing for a surgical operation must be carefully considered, and a massive bowel resection should always be prevented if at all possible.

Acknowledgments. We thank Hiroyuki Naora, MD, PhD, for advising on our results in genetic and biomolecular assays. This study was supported by Research on Intractable Diseases, Ministry of Health, Welfare, and Labor, Japan (#2141039040) (to T.K. and A.H.)

References

1. Pepin M, Schwarze U, Superti-Furga A, Byers PH. Clinical and genetic features of Ehlers–Danlos syndrome type IV, the vascular type. N Engl J Med 2000;342:673–80.
2. Watanabe A, Shimada T. The vascular type of Ehlers–Danlos syndrome. J Nippon Med Sch 2008;75:254–61.
3. Watanabe A, Kosho T, Wada T, Sakai N, Fujimoto M, Fukushima Y, et al. Genetic aspects of the vascular type of Ehlers–Danlos syndrome (vEDS, EDSIV) in Japan. Circ J 2007;71:261–5.
4. Yang JH, Lee ST, Kim JA, Kim SH, Jang SY, Ki CS, et al. Genetic analysis of three Korean patients with clinical features of Ehlers–Danlos syndrome type IV. J Korean Med Sci 2007;22:698–705.
5. Hata R, Kurata S, Shinkai H. Existence of malfunctioning pro a2(I) collagen genes in a patient with a pro a2(I)-chain-defective variant of Ehlers–Danlos syndrome. Eur J Biochem 1988;174: 231–7.
6. Hatamochi A, Ono M, Ueki H, Namba M. Regulation of collagen gene expression by transformed human fibroblasts: decreased type I and type III collagen RNA transcription. J Invest Dermatol 1991;96:473–7.
7. Fleischmajer R, Perlish JS, Krieg T, Timple R. Variability in collagen and fibronectin synthesis by scleroderma fibroblasts in primary culture. J Invest Dermatol 1981;76:400–3.
8. Okita H, Ikeda Y, Mitsuhashi Y, Namikawa H, Kitamura Y, Hamasaki Y, et al. A novel point mutation at donor splice-site in intron 42 of type III collagen gene resulting in the inclusion of 30 nucleotides into the mature mRNA in a case of vascular type of Ehlers–Danlos syndrome. Arch Dermatol Res 2009;302:395–9.
9. Matsushima K, Takara H. Endovascular treatment for a spontaneous rupture of the posterior tibial artery in a patient with Ehlers–Danlos syndrome type IV: report of a case. Surg Today 2009;39:523–6.
10. Freeman RK, Swegle J, Sise MJ. The surgical complications of Ehlers–Danlos syndrome. Am Surg 1996;62:869–73.
11. Privitera A, Milkhu C, Datta V, Sayegh M, Cohen R, Windsor A. Spontaneous rupture of the spleen in type IV Ehlers–Danlos syndrome: report of a case. Surg Today 2009;39(1):52–4.
12. Fuchs JR, Fishman SJ. Management of spontaneous colonic perforation in Ehlers–Danlos syndrome type IV. J Pediatr Surg 2004;39(2):e1–3.

nature genetics

Mutations affecting components of the SWI/SNF complex cause Coffin-Siris syndrome

Yoshinori Tsurusaki[1], Nobuhiko Okamoto[2], Hirofumi Ohashi[3], Tomoki Kosho[4], Yoko Imai[5], Yumiko Hibi-Ko[5], Tadashi Kaname[6], Kenji Naritomi[6], Hiroshi Kawame[7,8], Keiko Wakui[4], Yoshimitsu Fukushima[4], Tomomi Homma[9], Mitsuhiro Kato[10], Yoko Hiraki[11], Takanori Yamagata[12], Shoji Yano[13], Seiji Mizuno[14], Satoru Sakazume[15], Takuma Ishii[15,16], Toshiro Nagai[15], Masaaki Shiina[17], Kazuhiro Ogata[17], Tohru Ohta[18], Norio Niikawa[18], Satoko Miyatake[1], Ippei Okada[1], Takeshi Mizuguchi[1], Hiroshi Doi[1], Hirotomo Saitsu[1], Noriko Miyake[1] & Naomichi Matsumoto[1]

By exome sequencing, we found *de novo SMARCB1* mutations in two of five individuals with typical Coffin-Siris syndrome (CSS), a rare autosomal dominant anomaly syndrome. As *SMARCB1* encodes a subunit of the SWItch/Sucrose NonFermenting (SWI/SNF) complex, we screened 15 other genes encoding subunits of this complex in 23 individuals with CSS. Twenty affected individuals (87%) each had a germline mutation in one of six SWI/SNF subunit genes, including *SMARCB1*, *SMARCA4*, *SMARCA2*, *SMARCE1*, *ARID1A* and *ARID1B*.

Chromatin remodeling factors regulate the gene accessibility and expression by dynamic alteration of chromatin structure. SWI/SNF complexes have important roles in lineage specification, maintenance of stem cell pluripotency and tumorigenesis[1–5]. These complexes are composed of evolutionarily conserved core subunits and variant subunits. Brahma-associated factor (BAF) and Polybromo BAF (PBAF) complexes constitute two major subclasses[1–5]. It has been suggested that the BAF complex is similar to the yeast SWI/SNF complex and that the PBAF complex is more like the chromatin remodelling complex (RSC) in yeast, which is required for cell cycle progression through mitosis[6]. However, several subunits that are common to both BAF and PBAF complexes are predicted to be related to the regulation of lineage- and tissue-specific gene expression[2].

Coffin-Siris syndrome (MIM 135900) is a rare congenital anomaly syndrome characterized by growth deficiency, intellectual disability, microcephaly, coarse facial features and hypoplastic nail of the fifth finger and/or toe (**Fig. 1** and **Supplementary Table 1**)[7]. The majority of affected individuals represent sporadic cases, which is compatible with an autosomal dominant inheritance mechanism. The genetic cause for this syndrome has not been elucidated.

To identify the genetic basis of CSS, we performed whole-exome sequencing of five typical affected individuals (**Supplementary Methods**). Taking into account our model that assumes that an abnormality in a causal gene would be shared in two or more subjects, 51 variants were identified as candidates (**Supplementary Table 2**). All the variants were also examined by Sanger sequencing of PCR products amplified using genomic DNA from the five affected individuals and their parents. Nine variants were found to be false positives, 40 were inherited from either the father or mother, and 2 *de novo* heterozygous mutations of *SMARCB1* were found in 2 affected individuals (c.1130G>A (p.Arg377His) and c.1091_1093del AGA (p.Lys364del)) (**Table 1**, **Supplementary Fig. 1** and **Supplementary Methods**). Two *de novo* coding-sequence mutations occurring within a specific gene is an extremely unlikely event[8], supporting the idea that *SMARCB1* is a causative gene in CSS. Next, we screened *SMARCB1* in 23 individuals with CSS by high-resolution melting analysis[9] and identified the mutation encoding the p.Lys364del alteration in two additional individuals, including one of Arab descent (subject 22) (**Table 1** and **Supplementary Fig. 1**). As the mutation detection rate was relatively low (4 of 23, only 17.4%), we screened 15 additional genes encoding other SWI/SNF subunits (**Supplementary Table 3**). Unexpectedly, four other subunits, *SMARCA4* (also known as *BRG1*), *SMARCE1*, *ARID1A* and *ARID1B* were also found to be mutated (**Table 1** and **Supplementary Figs. 2–5**). In subject 10, a, c.2144C>T mutation in *ARID1B* (encoding p.Pro715Leu) was found in addition to the c.5632delG mutation in *ARID1B*. RT-PCR products that were amplified from total RNA from this subject's lymphoblastoid cells were cloned into the pCR4-TOPO vector. The two mutations were present on different alleles, according to sequencing of clones containing each allele (data not shown). As the c.5632delG mutation is

[1]Department of Human Genetics, Yokohama City University Graduate School of Medicine, Yokohama, Japan. [2]Division of Medical Genetics, Osaka Medical Center and Research Institute for Maternal and Child Health, Izumi, Japan. [3]Division of Medical Genetics, Saitama Children's Medical Center, Iwatsuki, Japan. [4]Department of Medical Genetics, Shinshu University School of Medicine, Matsumoto, Japan. [5]Division of Pediatrics, Japanese Red Cross Medical Center, Tokyo, Japan. [6]Department of Medical Genetics, University of the Ryukyus Faculty of Medicine, Okinawa, Japan. [7]Department of Genetic Counseling, Graduate School of Humanities and Sciences, Ochanomizu University, Tokyo, Japan. [8]Division of Medical Genetics, Nagano Children's Hospital, Azumino, Japan. [9]Division of Pediatrics, Yamagata Prefectural and Sakata Municipal Hospital Organization, Nihonkai General Hospital, Sakata, Japan. [10]Department of Pediatrics, Yamagata University Faculty of Medicine, Yamagata, Japan. [11]Hiroshima Municipal Center for Child Health and Development, Hiroshima, Japan. [12]Department of Pediatrics, Jichi Medical University, Tochigi, Japan. [13]Genetics Division, Department of Pediatrics, Los Angeles County and University of Southern California Medical Center, Keck School of Medicine, University of Southern California, Los Angeles, California, USA. [14]Department of Pediatrics, Central Hospital, Aichi Human Service Center, Kasugai, Japan. [15]Department of Pediatrics, Koshigaya Hospital, Dokkyo University School of Medicine, Koshigaya, Japan. [16]Nakagawa-No-Sato, Hospital for the Disabled, Saitama, Japan. [17]Department of Biochemistry, Yokohama City University Graduate School of Medicine, Yokohama, Japan. [18]Research Institute of Personalized Health Sciences, Health Sciences University of Hokkaido, Ishikari-Tobetsu, Japan. Correspondence should be addressed to N. Matsumoto (naomat@yokohama-cu.ac.jp) or N. Miyake (nmiyake@yokohama-cu.ac.jp).

Received 29 September 2011; accepted 10 February 2012; published online 18 March 2012; doi:10.1038/ng.2219

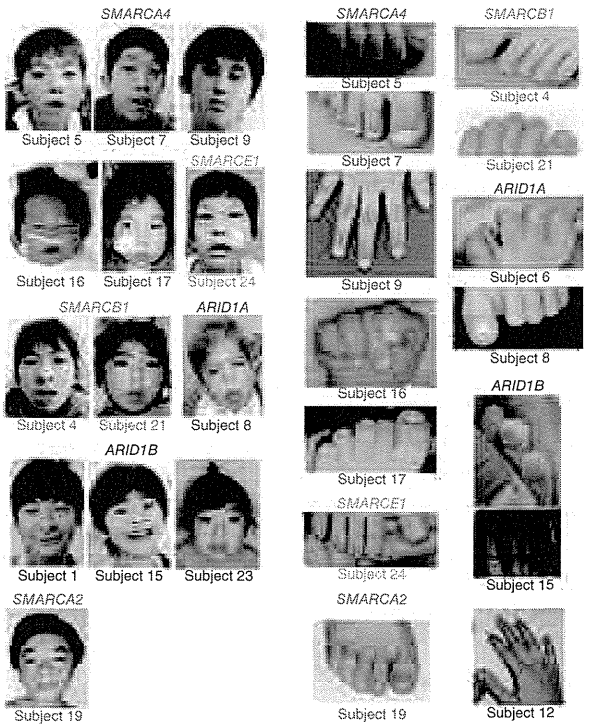

Figure 1 Photographs of individuals with Coffin-Siris syndrome. The faces (left) and hypoplastic-to-absent nail of the fifth finger or toe (right) of affected individuals are shown with the color-coded names of the corresponding mutated genes. The green arrow indicates the absence of the distal phalanx in the fifth toe. No obvious hypoplastic nails were observed in subjects 12 or 19. Consent for all the photographs was obtained from the families of the affected individuals.

very likely to be deleterious (as it results in a truncated protein), the c.2144C>T mutation is likely to be a rare polymorphism. Of note, subject 12, who presented an atypical facial appearance and indistinct hypoplastic nails, had two interstitial deletions at 6q25.3–q27 involving *ARID1B*, as detected by a SNP array (**Supplementary Fig. 6** and **Supplementary Methods**). Furthermore, subject 14 was found to have an interstitial deletion of *SMARCA2* by a SNP array (**Supplementary Fig. 7** and **Supplementary Methods**). No other copy-number changes involving genes encoding SWI/SNF complex components were found in subjects 2, 14 or 18 by array analysis. The overall mutation detection rate was 87%. In total, 20 of the 23 subjects had a mutation affecting one of the six SWI/SNF subunits.

Mutations in CSS were identified in the BAF-specific subunits *ARID1A* and *ARID1B* but not in PBAF-specific subunits (*BRD7*, *ARID2* and *PBRM1*) (**Supplementary Table 3**). In addition, mutations were identified in *SMARCA4* (*BRG1*) as well as in *SMARCA2* (*BRM*) (**Supplementary Table 3**). The BRG1 and BRM proteins are mutually exclusive catalytic ATP subunits in mammalian SWI/SNF complexes. Of note, the majority of heterozygous *Smarca4*-null mice survive with susceptibility to neoplasia, with a minority dying after birth because of exencephaly, whereas homozygous *Smarca2*-null mice are viable and fertile[4]. In *Smarca2*-null mice, Brg1 is upregulated, suggesting that Brg1 can functionally replace Brm in mice[10]. However, in humans, abnormalities in both *SMARCA4* and *SMARCA2* are found in CSS, indicating that the in-frame partial deletion of the gene encoding BRM in subject 19 has a specific mutational effect different from that of simple inactivation in mice. These data support the idea that abnormalities in the BRG1-BAF and BRM-BAF complexes can cause the abnormal neurological development in CSS.

All the mutated genes found in CSS, except for *SMARCE1*, have been reported to be associated with tumorigenesis[1,2]. Among the 23 subjects with CSS, only subject 3 with an *ARID1A* mutation presented with hepatoblastoma. To our knowledge, haploinsufficiency and/or homozygous inactivation of *ARID1A* have been found in several types of cancer but not in hepatoblastoma. Malignancies were not detected in any of the other subjects with CSS examined here. It remains to be seen whether malignancies are robustly associated with CSS.

Given the fact that all the mutations in *ARID1A* and *ARID1B* in CSS were predicted to cause protein truncation, we proposed that haploinsufficiency of these two genes must be able to cause CSS. cDNA analysis of lymphoblastoid cell lines from subjects 1, 6 and 23 indicated that the mutated transcripts were subject to nonsense-mediated mRNA decay (**Supplementary Fig. 8**). In subject 10, the *ARID1B* mutation associated with the creation of a premature stop codon in the last exon did not result in nonsense-mediated mRNA decay as expected (**Supplementary Fig. 8**).

In regard to the other mutated genes, germline heterozygous truncation mutations in *SMARCB1* and *SMARCA4* have been reported

Table 1 Mutations in individuals with Coffin-Siris syndrome

Subject ID	Gene	Mutation	Alteration	Type	Control allele frequency[a]
4	*SMARCB1*	c.1091_1093del AGA	p.Lys364del	*De novo*	0/502
11	*SMARCB1*	c.1130G>A	p.Arg377His	*De novo*	0/500
21	*SMARCB1*	c.1091_1093del AGA	p.Lys364del	NC	0/502
22	*SMARCB1*	c.1091_1093del AGA	p.Lys364del	NC	0/502
9	*SMARCA4*	c.1636_1638del AAG	p.Lys546del	*De novo*	0/350
7	*SMARCA4*	c.2576C>T	p.Thr859Met	*De novo*	0/368
5	*SMARCA4*	c.2653C>T	p.Arg885Cys	*De novo*	0/368
16	*SMARCA4*	c.2761C>T	p.Leu921Phe	*De novo*	0/368
25	*SMARCA4*	c.3032T>C	p.Met1011Thr	NC	0/372
17	*SMARCA4*	c.3469C>G	p.Arg1157Gly	*De novo*	0/368
19	*SMARCA2*	Partial deletion		*De novo*	–
24	*SMARCE1*	c.218A>G	p.Tyr73Cys	*De novo*	0/368
3	*ARID1A*	c.31_56del	p.Ser11Alafs*91	NC	0/330
6	*ARID1A*	c.2758C>T	p.Gln920*	NC	0/376
8	*ARID1A*	c.4003C>T	p.Arg1335*	*De novo*	–
1	*ARID1B*	c.1678_1688del	p.Ile560Glyfs*89	*De novo*	–
15	*ARID1B*	c.1903C>T	p.Gln635*	*De novo*	–
23	*ARID1B*	c.3304C>T	p.Arg1102*	*De novo*	–
10	*ARID1B*	c.2144C>T	p.Pro715Leu	NC	0/368
10	*ARID1B*	c.5632del G	p.Asp1878Metfs*96	NC	0/374
12	*ARID1B*	Microdeletion		NC	–

NC, not confirmed because parental samples were unavailable.
[a]The numbers indicate the observed allele frequency (alleles harboring the change/total tested alleles) in Japanese controls. None of the mutations was found in dbSNP132, the 1000 Genomes database or the National Heart, Lung, and Blood Institute (NHLBI) GO exomesequencing project database. –, not tested.

in individuals with rhabdoid tumor predisposition syndromes 1 (RTPS1; MIM 609322) and 2 (RTPS2; MIM 613325)[11,12], and various types of *SMARCB1* mutations (missense, in-frame deletion, nonsense and splice site) have been found in the germline of individuals with familial and sporadic schwannomatosis (MIM 162091)[13,14]. Furthermore, mice with heterozygous knockout of *Smarca4* or *Smarcb1* were prone to tumor development[2]. All the mutations in *SMARCA4* and *SMARCB1* in individuals with CSS were non-truncating (either missense or in-frame deletions), implying that they exert gain-of-function or dominant-negative effects (excluding haploinsufficiency as a cause). It is noteworthy that comparable germline mutations in *SMARCB1* have such different phenotypic consequences in their association with the phenotypes of CSS and schwannomatosis. The *SMARCB1* mutations in CSS and those in schwannomatosis are indeed different according to the Human Gene Mutation Database. With regard to the *SMARCA2* interstitial deletion in CSS, the change maintained the coding sequence reading frame but removed exons 20–27 that encode the HELICc domain. RT-PCR analysis confirmed the deletion of exons 20–27 at the cDNA level (**Supplementary Fig. 7**). These data suggest the importance of the HELICc domain in the SMARCA2 protein.

The various types of mutations in the genes encoding different SWI/SNF components resulted in similar CSS phenotypes. This suggests that the SWI/SNF complexes coordinately regulate chromatin structure and gene expression. This is the first report, to our knowledge, of germline mutations in SWI/SNF complex genes associated with a multiple congenital anomaly syndrome, highlighting new biological aspects of SWI/SNF complexes in humans. Similarly, genes encoding SNF2-related proteins, which are implicated as chromatin remodeling factors outside of SWI/SNF complexes, are mutated in different syndromes, including in α-thalassaemia/mental retardation syndrome X-linked (ATRX; *ATRX* mutations) and in coloboma, heart defect, atresia choanae, retarded growth and development, genital abnormality and ear abnormality (CHARGE) syndrome (*CHD7* haploinsufficiency)[3]. We expect that more mutations affecting chromatin remodeling factors will be found in different human diseases.

URLs. Human Gene Mutation Database, https://portal.biobase-international.com/cgi-bin/portal/login.cgi.

Note: Supplementary information is available on the Nature Genetics website.

ACKNOWLEDGMENTS

We thank all the family members for participating in this study. This work was supported by research grants from the Ministry of Health, Labour and Welfare (to N. Miyake, H.S. and N. Matsumoto), the Japan Science and Technology Agency (to N. Matsumoto), the Strategic Research Program for Brain Sciences (to N. Matsumoto), the Japan Epilepsy Research Foundation (to H.S.) and the Takeda Science Foundation (to N. Matsumoto and N. Miyake). This study was also funded by a Grant-in-Aid for Scientific Research on Innovative Areas (Foundation of Synapse and Neurocircuit Pathology) from the Ministry of Education, Culture, Sports, Science and Technology of Japan (to N. Matsumoto), a Grant-in-Aid for Scientific Research from the Japan Society for the Promotion of Science (to N. Matsumoto), a Grant-in-Aid for Young Scientists from the Japan Society for the Promotion of Science (to N. Miyake and H.S.) and a Grant for 2011 Strategic Research Promotion of Yokohama City University (to N. Matsumoto). This study was performed at the Advanced Medical Research Center at Yokohama City University. Informed consent was obtained from all the families of affected individuals. The Institutional Review Board of Yokohama City University approved this study.

AUTHOR CONTRIBUTIONS

Y.T., S. Miyatake, I.O., H.D., H.S. and N. Miyake performed exome sequencing and Sanger sequencing. Y.T., M.S., K.O., I.O., T.M., H.D., H.S. and N. Miyake performed data management and analysis. N.O., H.O., T. Kosho, Y.I., Y.H.-K., T. Kaname, K.N., H.K., K.W., Y.F., T.H., M.K., Y.H., T.Y., S.Y., S. Mizuno, S.S., T.I., T.N., T.O. and N.N. provided clinical materials after careful evaluation. Y.T., N. Miyake and N. Matsumoto wrote the manuscript. N. Matsumoto designed and oversaw all aspects of the study.

COMPETING FINANCIAL INTERESTS

The authors declare no competing financial interests.

Published online at http://www.nature.com/naturegenetics/.
Reprints and permissions information is available online at http://www.nature.com/reprints/index.html.

1. Reisman, D., Glaros, S. & Thompson, E.A. *Oncogene* **28**, 1653–1668 (2009).
2. Wilson, B.G. & Roberts, C.W. *Nat. Rev. Cancer* **11**, 481–492 (2011).
3. Clapier, C.R. & Cairns, B.R. *Annu. Rev. Biochem.* **78**, 273–304 (2009).
4. Bultman, S. *et al. Mol. Cell* **6**, 1287–1295 (2000).
5. Hargreaves, D.C. & Crabtree, G.R. *Cell Res.* **21**, 396–420 (2011).
6. Xue, Y. *et al. Proc. Natl. Acad. Sci. USA* **97**, 13015–13020 (2000).
7. Coffin, G.S. & Siris, E. *Am. J. Dis. Child.* **119**, 433–439 (1970).
8. Bamshad, M.J. *et al. Nat. Rev. Genet.* **12**, 745–755 (2011).
9. Wittwer, C.T., Reed, G.H., Gundry, C.N., Vandersteen, J.G. & Pryor, R.J. *Clin. Chem.* **49**, 853–860 (2003).
10. Reyes, J.C. *et al. EMBO J.* **17**, 6979–6991 (1998).
11. Schneppenheim, R. *et al. Am. J. Hum. Genet.* **86**, 279–284 (2010).
12. Taylor, M.D. *et al. Am. J. Hum. Genet.* **66**, 1403–1406 (2000).
13. Boyd, C. *et al. Clin. Genet.* **74**, 358–366 (2008).
14. Hadfield, K.D. *et al. J. Med. Genet.* **45**, 332–339 (2008).

CLINICAL GENETICS An International Journal of Genetics, Molecular and Personalized Medicine

Clin Genet 2013
Printed in Singapore. All rights reserved

CLINICAL GENETICS
doi: 10.1111/cge.12225

Short Report

Coffin–Siris syndrome is a SWI/SNF complex disorder

Tsurusaki Y, Okamoto N, Ohashi H, Mizuno S, Matsumoto N, Makita Y, Fukuda M, Isidor B, Perrier J, Aggarwal S, Dalal AB, Al-Kindy A, Liebelt J, Mowat D, Nakashima M, Saitsu H, Miyake N, Matsumoto N. Coffin–Siris syndrome is a SWI/SNF complex disorder.
Clin Genet 2013. © John Wiley & Sons A/S. Published by John Wiley & Sons Ltd, 2013

Coffin–Siris syndrome (CSS) is a congenital disorder characterized by intellectual disability, growth deficiency, microcephaly, coarse facial features, and hypoplastic or absent fifth fingernails and/or toenails. We previously reported that five genes are mutated in CSS, all of which encode subunits of the switch/sucrose non-fermenting (SWI/SNF) ATP-dependent chromatin-remodeling complex: *SMARCB1*, *SMARCA4*, *SMARCE1*, *ARID1A*, and *ARID1B*. In this study, we examined 49 newly recruited CSS-suspected patients, and re-examined three patients who did not show any mutations (using high-resolution melting analysis) in the previous study, by whole-exome sequencing or targeted resequencing. We found that *SMARCB1*, *SMARCA4*, or *ARID1B* were mutated in 20 patients. By examining available parental samples, we ascertained that 17 occurred *de novo*. All mutations in *SMARCB1* and *SMARCA4* were non-truncating (missense or in-frame deletion) whereas those in *ARID1B* were all truncating (nonsense or frameshift deletion/insertion) in this study as in our previous study. Our data further support that CSS is a SWI/SNF complex disorder.

Conflict of interest

None of the authors have any conflicts of interest to disclose.

Y Tsurusaki[a], N Okamoto[b], H Ohashi[c], S Mizuno[d], N Matsumoto[e], Y Makita[f], M Fukuda[g], B Isidor[h], J Perrier[i], S Aggarwal[j], AB Dalal[k], A Al-Kindy[l], J Liebelt[m], D Mowat[n], M Nakashima[a], H Saitsu[a], N Miyake[a] and N Matsumoto[a]

[a]Department of Human Genetics, Yokohama City University Graduate School of Medicine, Yokohama, Japan, [b]Division of Medical Genetics, Osaka Medical Center and Research Institute for Maternal and Child Health, Izumi, Japan, [c]Division of Medical Genetics, Saitama Children's Medical Center, Saitama, Japan, [d]Department of Pediatrics, Central Hospital, Aichi Human Service Center, Kasugai, Japan, [e]Department of Pediatrics, Asahikawa Medical University, Asahikawa Medical University, Asahikawa, Japan, [f]Education Center, Asahikawa Medical University, Asahikawa, Japan, [g]Department of Pediatrics, St. Marianna University School of Medicine, Kawasaki, Japan, [h]CHU Nantes, Service de Génétique Médicale, Nantes, France, [i]CHU Nantes, Service de Pédiatrie, Nantes, France, [j]Department of Medical Genetics, Nizam's Institute of Medical Sciences, Hyderabad, India, [k]Diagnostics Division, Centre for DNA Fingerprinting and Diagnostics, Hyderabad, India, [l]Department of Genetics, Sultan Qaboos University Hospital, Muscat, Oman, [m]South Australian Clinical Genetics Service, SA Pathology at Women's and Children's Hospital, North Adelaide, Australia, and [n]Department of Medical Genetics, Sydney Children's Hospital and the School of Women's and Children's Health, University of New South Wales, Sydney, Australia

Key words: Coffin–Siris syndrome – *ARID1B* – *SMARCA4* – *SMARCB1* – SWI/SNF ATP-dependent chromatin-remodeling complex

Corresponding author: Naomichi Matsumoto MD, PhD, Department of Human Genetics, Yokohama City University Graduate School of Medicine, 3-9 Fukuura, Kanazawa-ku, Yokohama 236-0004, Japan.
Tel.: +81 45 787 2606;
fax: +81 45 786 5219;
e-mail: naomat@yokohama-cu.ac.jp

Received 9 May 2013, revised and accepted for publication 28 June 2013

Coffin–Siris Syndrome (CSS; MIM 135900), first described by Coffin and Siris in 1970, is a congenital disorder characterized by intellectual disability (ID), growth deficiency, microcephaly, coarse facial features, and hypoplastic or absent fifth fingernails and/or toenails (1). Recently, we identified mutations in six genes encoding subunits of the switch/sucrose non-fermenting (SWI/SNF) ATP-dependent chromatin-remodeling complex: *SMARCB1*, *SMARCA4*, *SMARCA2*, *SMARCE1*, *ARID1A*, and *ARID1B* (2). Simultaneously, *SMARCA2* mutations were frequently found in patients with a similar syndrome, Nicolaides–Baraitser syndrome (NCBRS; MIM 601358) (3, 4). In fact, our patient with a *SMARCA2* mutation was clinically re-evaluated and recategorized as NCBRS (personal communication with Professor Raoul CM Hennekam of University of Amsterdam), removing *SMARCA2* as a causative gene for CSS.

Chromatin structure is important for the accessibility of DNA to transcription factors and for gene expression. The SWI/SNF complex modulates chromatin structure and plays important roles in transcription, cell differentiation, DNA repair, and tumor suppression (5, 6). The complexes contain a single ATPase subunit (SMARCA2 or SMARCA4), core subunits consisting of SMARCB1, SMARCC1, and SMARCC2, and form two major subclasses in mammals: BRG1/hBRM-associated factors (BAF) and polybromo-associated BAF (PBAF) complexes. ARID1A and ARID1B subunits are mutually exclusive and are only present in BAF complexes, whereas PBRM1, ARID2, and BRD7 subunits are PBAF-specific (7, 8). In our previous study, we identified CSS-related mutations in the BAF-specific subunits ARID1A and ARID1B (2).

In this study, we examined 49 newly recruited patients and re-examined three patients who did not show any mutation (by high-resolution melting analysis) in the previous study.

Materials and methods

Subjects and DNA preparation

We collected patients with suspected CSS showing most of core clinical features including ID, growth deficiency, coarse facial features, and hypoplastic/absent fifth fingernails and/or toenails (Fig. 1, Table 1). NCBRS, a similar condition to CSS (9), is excluded in this study. Genomic DNA of peripheral blood leukocytes was extracted by conventional methods. Detailed clinical information was obtained after written informed consent was secured from the family members (Table 1). The institutional review board of Yokohama City University School of Medicine approved this study.

Whole-exome sequencing and targeted resequencing

We performed whole-exome sequencing (WES) for 44 patients as previously described (10) and targeted resequencing in eight patients using a HaloPlex Target Enrichment System (Agilent Technologies, Santa Clara, CA) according to the manufacturer's protocol. A probe library was designed with oligonucleotide probes targeting 21 genes encoding SWI/SNF complex subunits (*ACTB, ACTL6A, ACTL6B, ARID1A, ARID1B, ARID2, BRD7, DPF1, DPF2, DPF3, PBRM1, PHF10, SMARCA2, SMARCA4, SMARCB1, SMARCC1, SMARCC2, SMARCD1, SMARCD2, SMARCD3,* and *SMARCE1*).

Priority scheme

Out of all variants within exons or ±2 bp from the exon–intron boundaries, those registered in dbSNP135, the 1000 Genomes Project, and the National Heart Lung and Blood Institute Exome Sequencing Project Exome Variant Server (NHLBI-ESP 5400), our in-house databases (408 exomes) or located within segmental duplications were removed.

Sanger sequencing

Variants were confirmed as true positives by Sanger sequencing on an ABI3500xl or ABI3130xl autosequencer (Life Technologies, Carlsbad, CA). Sequencing data were analyzed with Sequencher software (Gene Codes Corporation, Ann Arbor, MI). Parental samples were also confirmed (when available) to check the inheritance of variants.

Results

By WES, the mean coverage of RefSeq coding sequence was 49.6–175.6 reads, with 72.0–93.2%

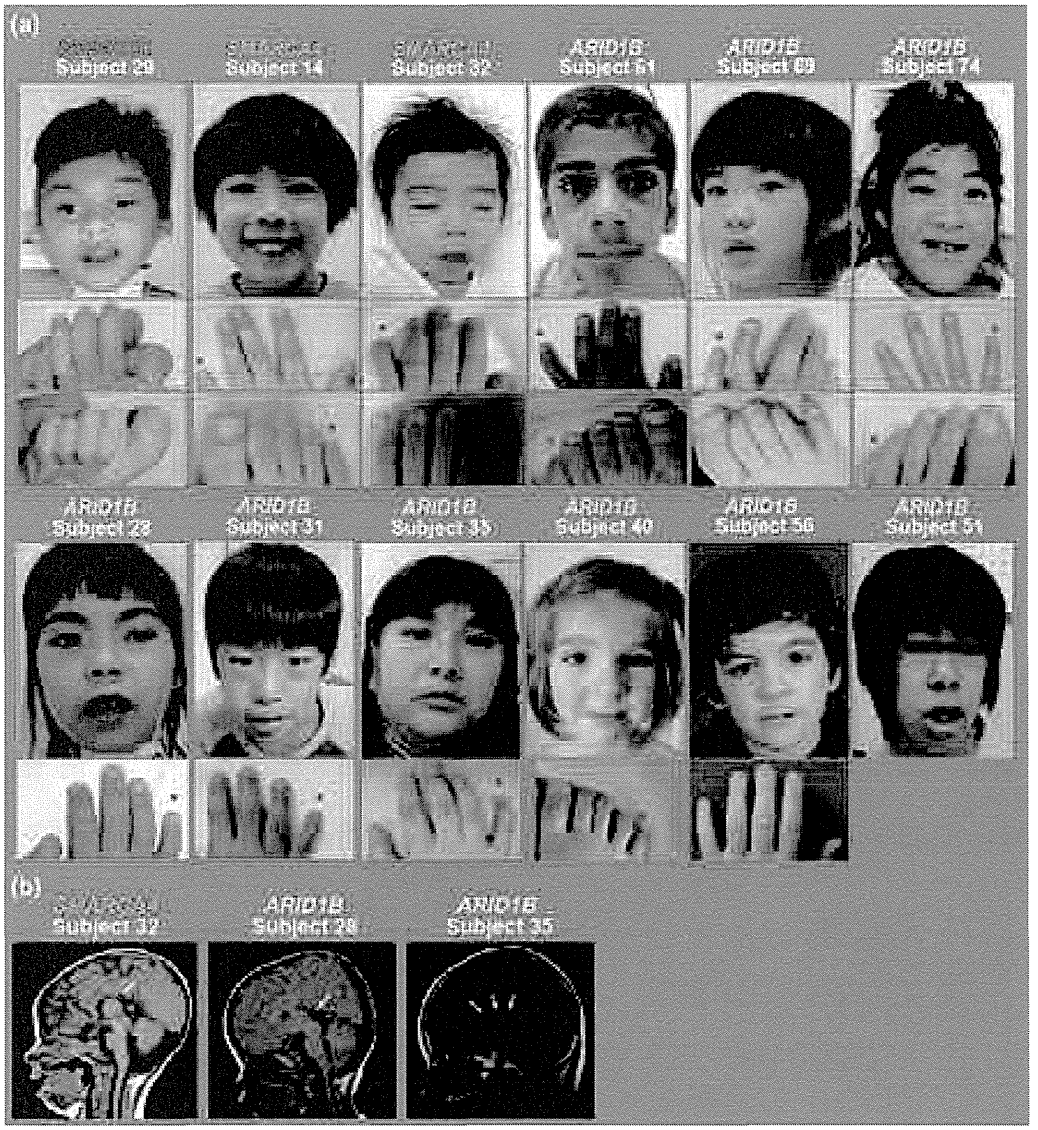

Fig. 1. Photographs and brain magnetic resonance imaging findings in patients with Coffin–Siris syndrome. (**a**) Faces (top) and nails of the fingers (middle) or/and toes (bottom) of patients, with the mutated gene indicated. Red asterisks indicate the fifth finger/toe. (**b**) T1-weighted midline sagittal magnetic resonance images. The individuals showed agenesis of the corpus callosum (arrows).

being covered by 20 or more reads. By targeted resequencing, the mean coverage of coding sequence in the target genes was 496.1–541.0 reads, with 96.5–97.2% being covered by 20 or more reads.

Mutations were discovered in *SMARCB1* (3 of 52 patients, 5.8%), *SMARCA4* (2 of 52 patients, 3.8%), and *ARID1B* (15 of 52 patients, 28.8%); all were confirmed by Sanger sequencing. We ascertained that a total of 17 mutations (among 20 patients) occurred *de novo*. No other pathological variants were found. In our previous study, mutations were found in *SMARCB1* (4 of 22 patients, 18.2%), *SMARCA4* (6 of 22 patients, 27.3%), *ARID1B* (5 of 22 patients, 22.7%), *ARID1A* (3 of 22 patients, 13.6%), and *SMARCE1* (1 of 22 patients, 4.5%). In this and our previous study, mutations in *SMARCB1* and *SMARCA4* were all non-truncating, implying that they exert gain-of-function or dominant negative effects whereas those in *ARID1B* mutations were all truncating, leading to haploinsufficiency (2). In total, 39 out of 71 CSS patients (54.9%) carry a mutation in one of five genes encoding a SWI/SNF complex subunit (Table 2; Figs S1 and S2). All the mutations are mutually exclusive.

Table 1. Clinical features in CSS

Clinical features	Mutated gene											Mutation positive	Mutation negative	Fischer's exact two-sided test *P* values[a]
	Tsurusaki et al. (2)					This study			Total					
	1B	B1	A4	1A	E1	1B	B1	A4	1B	B1	A4	All		
Neurodevelopment														
Developmental delay	5/5	4/4	6/6	3/3	1/1	15/15	1/1	2/2	20/20	5/5	8/8	37/37	8/8	1.000
Hypotonia	4/5	4/4	4/6	2/3	1/1	14/15	0/1	1/2	18/20	4/5	5/8	30/37	7/8	1.000
Microcephaly	1/5	2/3	4/5	1/3	1/1	2/15	1/1	0/2	3/20	3/4	4/7	12/35	3/8	1.000
Small cerebellum	0/5	2/3	0/3	1/2		1/15	0/1	1/2	1/20	2/4	1/5	5/31	0/6	0.567
Seizures	2/5	2/4	2/6	0/2		5/15	1/1	0/2	7/20	3/5	2/8	12/35	4/8	0.443
Dandy–Walker	0/5	0/2	1/5	1/3		1/14	0/1	1/2	1/19	0/3	2/7	4/32	0/7	1.000
Abnormal corpus callosum	1/2	2/2	1/1	3/3		6/13	0/1	1/2	7/15	2/3	2/3	14/24	2/6	0.378
Vision problem	1/4	2/3	5/6	1/2		2/15	0/1	0/2	3/19	2/4	5/8	11/33	3/7	0.679
Hearing loss	1/5	3/4	3/6	1/2	1/1	1/15	1/1	1/2	2/20	4/5	4/8	12/36	0/7	0.163
Ectodermal														
Absent/hypoplastic fifth finger/toenails	5/5	4/4	6/6	3/3	1/1	11/15	1/1	2/2	16/20	5/5	8/8	33/37	4/7	0.068
Hirsutism	5/5	3/4	6/6	3/3	1/1	14/15	1/1	2/2	19/20	4/5	8/8	35/37	7/7	1.000
Sparse scalp hair	3/5	4/4	3/6	3/3	1/1	7/15	1/1	1/2	10/20	5/5	4/8	23/37	1/7	0.035
Thick eyebrow	5/5	4/4	6/6	2/3	1/1	15/15	1/1	2/2	20/20	5/5	8/8	36/37	8/8	1.000
Long eyelashes	4/5	4/4	6/6	3/3	1/1	13/15	1/1	2/2	17/20	5/5	8/8	34/37	7/8	0.557
Abnormal/delayed dentition	5/5	3/3	3/5	2/2	1/1	4/10	1/1	0/1	9/15	4/4	3/6	19/28	0/6	0.004
Non-functioning/absent tear duct	0/1	2/3	1/4	0/2	0/1	2/14	0/1	0/2	2/15	2/4	1/6	5/28	0/7	0.559
Facial														
Coarse appearance	5/5	4/4	6/6	3/3	1/1	15/15	1/1	2/2	20/20	5/5	8/8	37/37	8/8	1.000
Flat nasal bridge	5/5	3/4	4/6	2/3	1/1	12/15	1/1	2/2	17/20	4/5	6/8	30/37	6/8	0.652
Broad nose	5/5	4/4	2/6	2/3	1/1	13/15	1/1	2/2	18/20	5/5	4/8	30/37	6/8	0.652
Wide mouth	3/5	4/4	3/6	3/3	1/1	13/15	1/1	2/2	16/20	5/5	5/8	30/37	6/8	0.652
Thick lips	5/5	4/4	5/6	3/3	1/1	15/15	1/1	2/2	20/20	5/5	7/8	36/37	8/8	1.000
Abnormal ears	4/5	4/4	5/6	3/3	1/1	9/15	1/1	2/2	13/20	5/5	7/8	29/37	1/7	0.002
High palate	5/5	4/4	5/5	2/3	1/1	9/15	1/1	2/2	14/20	5/5	7/7	29/36	6/8	0.659
Cleft palate	0/5	2/4	3/6	2/3	1/1	1/15	0/1	1/2	1/20	2/5	4/8	10/37	0/8	0.169
Ptosis	0/5	3/4	5/6	0/3	1/1	3/15	0/1	1/2	3/20	3/5	6/8	13/37	3/8	1.000
Macroglossia	0/5	3/4	2/6	0/3	1/1	2/15	0/1	0/2	2/20	3/5	2/8	8/37	0/7	0.318
Short philtrum	0/5	0/4	3/6	1/3	1/1	6/15	1/1	1/2	6/20	1/5	4/8	13/37	1/8	0.402
Long philtrum	1/5	2/4	0/6	1/3	0/1	5/12	0/1	0/1	6/17	2/5	0/7	9/33	1/8	0.653
Skeletal														
Absent/hypoplastic fifth phalanx (hand)	5/5	1/1	4/5	2/2	1/1	5/14		2/2	10/19	1/1	6/7	20/30	2/8	0.050
Absent/hypoplastic fifth phalanx (foot)	4/5	1/1	3/3	2/2	1/1	7/12		2/2	11/17	1/1	5/5	20/26	3/7	0.161
Short stature	2/5	4/4	4/5	2/3	1/1	10/14	1/1	1/2	12/19	5/5	5/7	25/35	6/8	1.000
Spinal anomalies	3/4	3/4	1/4	1/2	1/1	3/14	1/1	0/2	6/18	4/5	1/6	13/32	3/7	1.000
Delayed bone age	0/1	1/1		1/2		2/11		0/1	2/12	1/1	0/1	4/16	4/6	0.137

Table 1. Continued.

Clinical features	Mutated gene										Mutation positive	Mutation negative	Fischer's exact two-sided test *P* values[a]
	Tsurusaki et al. (2)					This study			Total				
	1B	B1	A4	1A	E1	1B	B1	A4	1B	B1	A4	All		
Gastrointestinal														
Feeding problems	4/5	4/4	5/6	3/3	1/1	10/15	1/1	2/2	14/20	5/5	7/8	30/37	6/7	1.000
Sucking problems	4/5	4/4	5/6	3/3		11/15	1/1	2/2	15/20	5/5	7/8	30/36	6/8	0.623
Intestinal anomalies	1/5	1/4	2/5	2/2		1/15	0/1	0/2	2/20	1/5	2/7	7/34	1/6	1.000
Tumor	0/5	0/4	0/6	1/3	0/1	0/15	0/1	0/2	0/20	0/5	0/8	1/37	0/5	1.000
Others														
Frequent infections	5/5	3/4	4/6	3/3	1/1	6/15	1/1	1/2	11/20	4/5	5/8	24/37	4/7	0.692
IUGR	1/5	2/4	2/6	1/3	1/1	6/15	1/1	2/2	7/20	3/5	4/8	16/37	3/8	1.000
Joint laxity	2/4	2/3	2/6	2/3	1/1	7/15	1/1	1/2	9/19	3/4	3/8	18/35	4/8	1.000
Cardiac findings	1/5	2/4	2/6	3/3	1/1	3/15	0/1	0/2	4/20	2/5	2/8	12/37	2/6	1.000
Genital findings	1/4	1/2	1/6	1/2	0/1	1/15	1/1	0/2	2/19	2/3	1/8	6/33	0/5	0.570
Inguinal hernia	0/5	2/4	2/6	1/3	0/1	0/15	1/1	1/2	0/20	3/5	3/8	7/37	1/8	1.000
Umbilical hernia	0/4	0/4	1/6	0/3	0/1	0/15	1/1	1/2	0/19	1/5	2/8	3/36	1/8	0.566
Renal findings	0/4	0/3	0/4	0/2	0/1	2/13	1/1	0/2	2/17	1/4	0/6	3/30	0/5	1.000
Diaphragmatic hernia	0/5	1/4	0/5	0/3	0/1	0/15	0/1	0/2	0/20	1/5	0/7	1/36	0/8	1.000

CSS, Coffin–Siris syndrome, 1B, *ARID1B*; B1, *SMARCB1*; A4, *SMARCA4*; 1A, *ARID1A*; E1, *SMARCE1*. IUGR, Intrauterine growth restriction

[a]*P* values for deviation from expected distribution of mutation-positive and mutation-negative subjects.

Discussion

On the basis of this and our previous mutation survey, the mutation detection rates in CSS are 54.9% (39 out of 71) and *ARID1B* mutations are the most common genetic cause of CSS (20 of 71 patients, 28.2%). Santen et al. also found truncating mutations of *ARID1B* in three CSS patients by WES (11). All *ARID1B* mutations reported in CSS are truncating (Figs S1 and S2). Interestingly, Hoyer et al. also reported that *ARID1B* truncating mutations are a frequent cause of unspecific moderate-severe ID (12) (Fig. S1). All of the mutations found in ID were truncating. Some ID patients showed characteristic coarse facial features similar to CSS. Furthermore, hypoplastic/absent fifth finger/toe nails have been described in some ID patients (12). Therefore, taking into consideration the symptoms of CSS, some of the ID patients may also have CSS or these patients and CSS patients are phenotypically overlapped.

We tried to find characteristic clinical features of CSS specific to particular mutated genes. It is only noted that all the CSS patients with *SMARCB1, SMARCA4, ARID1A* or *SMARCE1* mutations showed hypoplastic/absent fifth finger/toe nails, but some patients with *ARID1B* mutations did not. Except for that, it is difficult to clinically differentiate patients by mutant genes partly due to variable phenotypes in CSS. These findings may suggest that different subunits of the SWI/SNF complex coordinately regulate chromatin and gene expression as a functional unit (13).

Clinical features were compared between patients with identified mutations of genes encoding a SWI/SNF complex subunit and patients without identified SWI/SNF complex subunit mutations using Fisher's exact test (Table 1). Four clinical features showed significant difference including sparse scalp hair ($P = 0.035$), abnormal/delayed dentition ($P = 0.004$), abnormal ears ($P = 0.002$), and absent/hypoplastic fifth phalanx of the hand ($P = 0.050$), although the number of mutation-negative patients is small.

The SWI/SNF complex plays an important role in tumor suppression (7). Mutations in *SMARCB1* were first reported in human cancer (14, 15). Most mutations in *SMARCB1* were truncating mutations and were mainly found in malignant rhabdoid tumors (MRTs) somatically and in the germ line. Furthermore, germ line mutations in *SMARCB1* were also found in schwannomatosis. The *SMARCB1* mutations arise somatically or in the germ line, the second allele was also altered by copy neutral loss of heterozygosity (LOH) as a second hit in the tumor cells. In addition, one family with MRTs was reported as having a germ line nonsense mutation in *SMARCA4* (14, 16). This nonsense mutation is not found in mRNA of immortalized B cells, indicating nonsense-mediated mRNA decay as the molecular mechanism for the lack of *SMARCA4* expression together with copy neutral LOH encompassing *SMARCA4* as a second hit in the tumor cells. To date, these patients having tumors with germline mutations in *SMARCB1* or *SMARCA4*

Table 2. Mutations found in patients with Coffin–Siris syndrome

Patient ID	Gene	RefSeq accession number	Nucleotide change	Amino acid change	Mutation	Type	Reference
4	*SMARCB1*	NM_003073.3	c.1091_1093del	p.Lys364del	Inframeshift	*de novo*	Tsurusaki et al. (2)
21	*SMARCB1*	NM_003073.3	c.1091_1093del	p.Lys364del	Inframeshift	nc	Tsurusaki et al. (2)
22	*SMARCB1*	NM_003073.3	c.1091_1093del	p.Lys364del	Inframeshift	nc	Tsurusaki et al. (2)
29	*SMARCB1*	NM_003073.3	c.1091_1093del	p.Lys364del	Inframeshift	*de novo*	This report
37	*SMARCB1*	NM_003073.3	c.1091_1093del	p.Lys364del	Inframeshift	*de novo*	This report
48	*SMARCB1*	NM_003073.3	c.1091_1093del	p.Lys364del	Inframeshift	*de novo*	This report
11	*SMARCB1*	NM_003073.3	c.1130G>A	p.Arg377His	Missense	*de novo*	Tsurusaki et al. (2)
32	*SMARCA4*	NM_001128849.1	c.1372_1395del	p.Lys458_Glu465del	Inframeshift	*de novo*	This report
9	*SMARCA4*	NM_001128849.1	c.1636_1638del	p.Lys546del	Inframeshift	*de novo*	Tsurusaki et al. (2)
7	*SMARCA4*	NM_001128849.1	c.2576C>T	p.Thr859Met	Missense	*de novo*	Tsurusaki et al. (2)
5	*SMARCA4*	NM_001128849.1	c.2653C>T	p.Arg885Cys	Missense	*de novo*	Tsurusaki et al. (2)
14	*SMARCA4*	NM_001128849.1	c.2654G>A	p.Arg885His	Missense	*de novo*	This report
16	*SMARCA4*	NM_001128849.1	c.2761C>T	p.Leu921Phe	Missense	*de novo*	Tsurusaki et al. (2)
25	*SMARCA4*	NM_001128849.1	c.3032T>C	p.Met1011Thr	Missense	*de novo*	Tsurusaki et al. (2)
17	*SMARCA4*	NM_001128849.1	c.3469C>G	p.Arg1157Gly	Missense	*de novo*	Tsurusaki et al. (2)
38	*ARID1B*	NM_020732.3	c.1389_1398del	p.Ala464Serfs*35	Frameshift	*de novo*	This report
28	*ARID1B*	NM_020732.3	c.1392_1402del	p.Gln467Argfs*64	Frameshift	*de novo*	This report
1	*ARID1B*	NM_020732.3	c.1678_1688del	p.Ile560Glyfs*89	Frameshift	*de novo*	Tsurusaki et al. (2)
40	*ARID1B*	NM_020732.3	c.1713del	p.Gly572Glufs*21	Frameshift	*de novo*	This report
15	*ARID1B*	NM_020732.3	c.1903C>T	p.Gln635*	Nonsense	*de novo*	Tsurusaki et al. (2)
61	*ARID1B*	NM_020732.3	c.2062del	p.Leu688Serfs*9	Frameshift	*de novo*	This report
75	*ARID1B*	NM_020732.3	c.2891_2892insAC	p.Phe964Leufs*5	Frameshift	*de novo*	This report
23	*ARID1B*	NM_020732.3	c.3304C>T	p.Arg1102*	Nonsense	*de novo*	Tsurusaki et al. (2)
53	*ARID1B*	NM_020732.3	c.3481G>T	p.Glu1161*	Nonsense	*de novo*	This report
74	*ARID1B*	NM_020732.3	c.4009C<T	p. Arg1337*	Nonsense	nc	This report
56	*ARID1B*	NM_020732.3	c.4820_4825delinsAGGCT	p.Thr1607Lysfs*7	Frameshift	*de novo*	This report
69	*ARID1B*	NM_020732.3	c.4821del	p.Pro1609Leufs*5	Frameshift	*de novo*	This report
27	*ARID1B*	NM_020732.3	c.4911G>A	p.Trp1637*	Nonsense	*de novo*	This report
34	*ARID1B*	NM_020732.3	c.4916_4917del	p.Val1639Aspfs*5	Frameshift	*de novo*	This report
35	*ARID1B*	NM_020732.3	c.5623_5625delinsTGACGTCT	p.Ala1875*	Nonsense	nc	This report
10	*ARID1B*	NM_020732.3	c.5632del	p.Asp1878Metfs*96	Frameshift	nc	Tsurusaki et al. (2)
51	*ARID1B*	NM_020732.3	c.6120C>G	p.Tyr2040*	Nonsense	nc	This report
31	*ARID1B*	NM_020732.3	c.6382C>T	p.Arg2128*	Nonsense	*de novo*	This report
55	*ARID1B*	NM_020732.3	c.6516C>G	p.Tyr2172*	Nonsense	*de novo*	This report
12	*ARID1B*	NM_020732.3			Microdeletion	nc	Tsurusaki et al. (2)
3	*ARID1A*	NM_006015.4	c.31_56del	p.Ser11Alafs*91	Frameshift	nc	Tsurusaki et al. (2)
6	*ARID1A*	NM_006015.4	c.2758C>T	p.Gln920*	Nonsense	nc	Tsurusaki et al. (2)
8	*ARID1A*	NM_006015.4	c.4003C>T	p.Arg1335*	Nonsense	*de novo*	Tsurusaki et al. (2)
24	*SMARCE1*	NM_003079.4	c.218A>G	p.Tyr73Cys	Missense	*de novo*	Tsurusaki et al. (2)

nc, not confirmed, as parental samples were unavailable.

have not been reported in association with the CSS phenotype. It is still unclear why germ line mutations in the same genes can give rise to CSS or different types of tumors. Heterozygous knockout mice were born and appeared normal, but these mice started developing tumors (14). In human, *SMARCB1* and *SMARCA4* mutations in CSS patients were all missense mutations or in-frame deletion while the majority of patients with tumors showed truncating mutations. These evidences might indicate that mutations in CSS were a gain-of-function or a dominant-negative type while those in patients with tumors resulted in the loss of function. Tumor formation was only found in one of our CSS patients carrying an *ARID1A* mutation, who presented with hepatoblastoma and carried an *ARID1A* mutation (2) (Table 1). Mutations in *ARID1A* are undoubtedly involved in the formation of various tumors, but unfortunately autopsy was not performed in the CSS patient and the tumor tissue was unavailable. Furthermore, germline mutations of *ARID1A* have been unreported in relation to patients with tumors so far. Careful follow-ups should be undertaken to monitor potential tumor development in these CSS patients.

In conclusion, we identified mutations in *SMARCB1, SMARCA4,* and *ARID1B* in 20 out of 52 CSS-suspected patients using WES or targeted resequencing. Further investigation of more patients is necessary to validate phenotype–genotype correlations and tumor susceptibility. In yeast, function of SWI/SNF complex is well characterized. SWI/SNF complexes interact with some transcription factors and regulate the expression of hundreds of genes (6), suggesting that other upstream or downstream genes may be mutated in CSS. Further research is needed to understand the pathomechanism of CSS.

Supporting Information

The following Supporting information is available for this article:

Fig.S1 Protein structure of SMARCB1, SMARCA4, and ARID1B with functional domains. Mutations identified in this study are indicated above the structure, and those identified in the previous study and other studies corresponding to Coffin–Siris syndrome or ID (11, 12) are indicated below the structure. SMARCB1 contains two sucrose non-fermenting 5 (SNF5) domains. SMARCA4 contains a conserved Gln, Leu, Gln (QLQ) motif, a helicase/SANT-associated (HSA) domain, a Brahma and Kismet (BRK) domain, DEAD-like helicases superfamily (DEXDc) and helicase superfamily c-terminal (HELICc) domains, and a bromodomain (BROMO). ARID1B contains an ARID/BRIGHT DNA-binding (ARID) domain.
Fig.S2 Number of Coffin–Siris syndrome patients with a mutation in each SWI/SNF complex subunit gene.

Additional Supporting information may be found in the online version of this article.

Acknowledgments

We thank the patients and their families for participating in this work. We also thank Ms. N. Watanabe for technical assistance. This work was supported by Ministry of Health, Labour, and Welfare (H. S., N. Miyake and N. Matsumoto), the Japan Science and Technology Agency (N. Matsumoto), the Strategic Research Program for Brain Sciences (N. Matsumoto) and a Grant-in-aid for Scientific Research on Innovative Areas-(Transcription cycle)-from the Ministry of Education, Culture, Sports, Science, and Technology of Japan (N. Miyake and N. Matsumoto), a Grant-in-aid for Scientific Research from the Japan Society for the Promotion of Science (N. Matsumoto), a Grant-in-aid for Young Scientists from the Japan Society for the Promotion of Science (H. S., N. Miyake and N. Matsumoto), and a grant from the Takeda Science Foundation (N. Miyake and N. Matsumoto).

References

1. Coffin GS, Siris E. Mental retardation with absent fifth fingernail and terminal phalanx. Am J Dis Child 1970: 119: 433–439.
2. Tsurusaki Y, Okamoto N, Ohashi H et al. Mutations affecting components of the SWI/SNF complex cause Coffin–Siris syndrome. Nat Genet 2012: 44: 376–378.
3. Van Houdt JK, Nowakowska BA, Sousa SB et al. Heterozygous missense mutations in SMARCA2 cause Nicolaides-Baraitser syndrome. Nat Genet 2012: 44: 445–449.
4. Wolff D, Endele S, Azzarello-Burri S et al. In-frame deletion and missense mutations of the C-terminal helicase domain of SMARCA2 in three patients with Nicolaides–Baraitser syndrome. Mol Syndromol 2012: 2: 237–244.
5. Amankwah EK, Thompson RC, Nabors LB et al. SWI/SNF gene variants and glioma risk and outcome. Cancer Epidemiol 2013: 37: 162–165.
6. Santen GW, Kriek M, van Attikum H. SWI/SNF complex in disorder: SWItching from malignancies to intellectual disability. Epigenetics 2012a: 7: 1219–1224.
7. Wilson BG, Roberts CW. SWI/SNF nucleosome remodellers and cancer. Nat Rev Cancer 2011: 11: 481–492.
8. Euskirchen G, Auerbach RK, Snyder M. SWI/SNF chromatin-remodeling factors: multiscale analyses and diverse functions. J Biol Chem 2012: 287: 30897–30905.
9. Castori M, Covaciu C, Rinaldi R et al. A rare cause of syndromic hypotrichosis: Nicolaides–Baraitser syndrome. J Am Acad Dermatol 2008: 59: S92–98.
10. Saitsu H, Nishimura T, Muramatsu K et al. De novo mutations in the autophagy gene WDR45 cause static encephalopathy of childhood with neurodegeneration in adulthood. Nat Genet 2013: 45: 445–449.
11. Santen GW, Aten E, Sun Y et al. Mutations in SWI/SNF chromatin remodeling complex gene ARID1B cause Coffin–Siris syndrome. Nat Genet 2012b: 44: 379–380.
12. Hoyer J, Ekici AB, Endele S et al. Haploinsufficiency of ARID1B, a member of the SWI/SNF-a chromatin-remodeling complex, is a frequent cause of intellectual disability. Am J Hum Genet 2012: 90: 565–572.
13. Ronan JL, Wu W, Crabtree GR. From neural development to cognition: unexpected roles for chromatin. Nat Rev Genet 2013: 14: 347–359.
14. Romero OA, Sanchez-Cespedes M. The SWI/SNF genetic blockade: effects in cell differentiation, cancer and developmental diseases. Oncogene 2013: Epub ahead of print.
15. Versteege I, Sevenet N, Lange J et al. Truncating mutations of hSNF5/INI1 in aggressive paediatric cancer. Nature 1998: 394: 203–206.
16. Schneppenheim R, Fruhwald MC, Gesk S et al. Germline nonsense mutation and somatic inactivation of SMARCA4/BRG1 in a family with rhabdoid tumor predisposition syndrome. Am J Hum Genet 2010: 86: 279–284.

RESEARCH LETTER

AMERICAN JOURNAL OF medical genetics PART A

Prenatal Genetic Testing for a Microdeletion at Chromosome 14q32.2 Imprinted Region Leading to UPD(14)pat-like Phenotype

Aiko Sasaki,[1] Masahiro Sumie,[1] Seiji Wada,[1] Rika Kosaki,[2] Kenji Kuroswa,[3] Maki Fukami,[4] Haruhiko Sago,[1] Tsutomu Ogata,[5] and Masayo Kagami[4]*

[1]Department of Maternal-Fetal and Neonatal Medicine, National Center for Child Health and Development, Tokyo, Japan

[2]Division of Medical Genetics, National Center for Child Health and Development, Tokyo, Japan

[3]Division of Medical Genetics, Kanagawa Children's Medical Center, Yokohama, Japan

[4]Department of Molecular Endocrinology, National Research Institute for Child Health and Development, Tokyo, Japan

[5]Department of Pediatrics, Hamamatsu University School of Medicine, Hamamatsu, Japan

Manuscript Received: 17 April 2013; Manuscript Accepted: 16 July 2013

TO THE EDITOR:

Human chromosome 14q32.2 imprinted region carries several paternally expressed genes (*PEGs*) such as *DLK1* and *RTL1* and maternally expressed genes (*MEGs*) such as *MEG3* (alias, *GTL2*) and *RTL1as* (*RTL1 antisense*), together with the germline-derived primary *DLK1-MEG3* intergenic differentially methylated region (IG-DMR) and the postfertilization-derived secondary *MEG3*-DMR (Fig. 1) [da Rocha et al., 2008; Kagami et al., 2008a]. Consistent with this, paternal uniparental disomy 14 (UPD(14) results in a unique phenotype characterized by facial abnormality, small bell-shaped thorax, abdominal wall defects, placentomegaly, and polyhydramnios [Kagami et al., 2005, 2008a,b]. In this regard, we have recently reported that heterozygous microdeletions and epimutations (hypermethylations) affecting unmethylated DMR (s) of maternal origin also lead to UPD(14)pat-like phenotype [Kagami et al., 2008a, 2010, 2012]. Indeed, after studying 26 patients with UPD(14)pat-like phenotype, we identified UPD (14)pat in 17 patients (65.4%), microdeletions in 5 patients (19.2%), and epimutations in 4 patients (15.4%) [Kagami et al., 2012]. Importantly, although there is no report describing recurrence of UPD(14)pat and epimutation in familial members with a normal karyotype, microdeletions can be transmitted recurrently from mothers with the same heterozygous microdeletions to offsprings [Kagami et al., 2008a]. Here, we report on our experience of a prenatal genetic testing for a microdeletion at the chromosome 14q32.2 imprinted region.

A 33-year-old Japanese woman came to us with her husband seeking for prenatal diagnosis of a fetus at 9 weeks of gestation. The first child and the mother have been reported previously as cases 3 and 11 of Family B in Kagami et al. [2008a]. In brief, the child had upd(14)pat-like phenotype and a maternally derived 411,354 bp microdeletion involving *WDR25*, *BEGAIN*, *DLK1*, *MEG3*, *RTL1/RTL1as*, and *MEG8* (Fig. 1). The mother had UPD(14)mat-like phenotype and the same microdeletion on the paternally derived chromosome 14. The parents hoped to deliver the fetus at a local hospital if there is no microdeletion or at our hospital with a neonatal intensive care unit if a microdeletion is identified.

After thorough consultation, we performed trans-abdominal chorionic villus sampling (CVS) at 12 weeks of gestation. Immediately after the sampling, fluorescence in situ hybridization was carried out with an RP11-566J3 probe detecting a segment within

How to Cite this Article:
Sasaki A, Sumie M, Wada S, Kosaki R, Kuroswa K, Fukami M, Sago H, Ogata T, Kagami M. 2013. Prenatal Genetic Testing for a Microdeletion at Chromosome 14q32.2 Imprinted Region Leading to UPD(14)pat-like Phenotype.
Am J Med Genet Part A 9999:1–3.

Conflict of interest: none.
Grant sponsor: Scientific Research (A); Grant numbers: 22249010, 25253023; Grant sponsor: Research (B); Grant number: 21028026; Grant sponsor: Japan Society for the Promotion of Science; Grant sponsor: Research on Intractable Diseases; Grant number: H22-161; Grant sponsor: National Center for Child Health and Development; Grant numbers: 23A-1, 25-10; Grant sponsor: Takeda Science Foundation; Grant sponsor: Novartis Foundation; Grant sponsor: The Japan and Foundation for Pediatric Research.
*Correspondence to:
Masayo Kagami, M.D, Ph.D, Department of Molecular Endocrinology, National Research Institute for Child Health and Development, Tokyo 157-8535, Japan. E-mail: kagami-ms@ncchd.go.jp
Article first published online in Wiley Online Library (wileyonlinelibrary.com): 00 Month 2013
DOI 10.1002/ajmg.a.36185

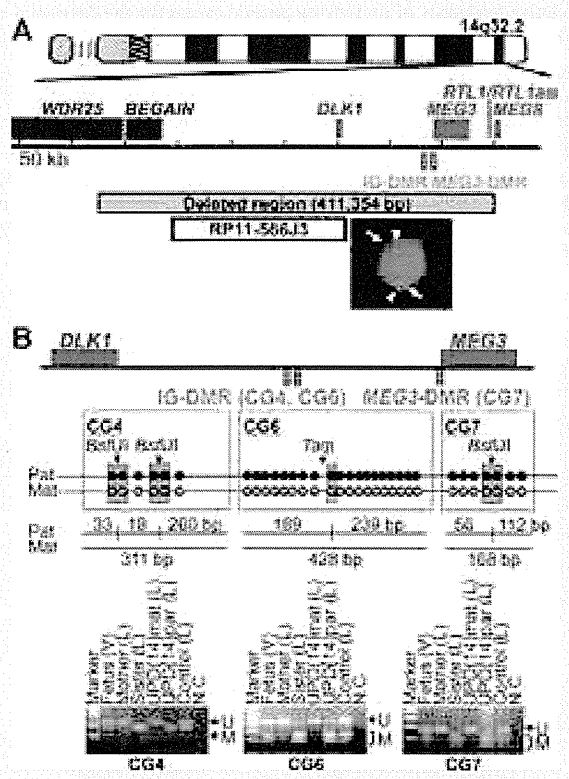

FIG. 1. Summary of the molecular studies. A: The physical map of the 14q32.2 imprinted region and the FISH finding of the fetus. *PEGs* are shown in blue, *MEGs* in red, and the IG-DMR and the *MEG3*-DMR in green. The gray rectangle indicates the 411,354 bp microdeletion identified in the first child and the mother, and the white rectangle denotes the region detected by the RP11-566J3 BAC probe. The FISH analysis reveals two red signals (arrows) identified by the RP11-566J3 BAC probe and two green signals (arrowheads) detected by the RP11-566I2 BAC probe for 14q12 utilized as an internal control. B: The methylation analysis for the IG-DMR (CG4 and CG6) and the *MEG3*-DMR (CG7) by COBRA. The black and white circles indicate methylated and unmethylated cytosines at the CpG dinucleotides, respectively. Pat: paternally derived chromosome; and Mat: maternally derived chromosome. PCR products for CG4 (311 bp) are digested with *Bst*UI into three fragments (33, 18, and 260 bp) when cytosines at the first and the second CpG dinucleotides and the fourth and fifth CpG dinucleotides (indicated with orange rectangles) are methylated. The PCR products for CG6 (428 bp) are digested with *Taq*I into two fragments (189 and 239 bp) when the cytosine at the 9th CpG dinucleotide (indicated with an orange rectangle) is methylated. The PCR products of CG7 (168 bp) are digested with *Bst*UI into two fragments (56 and 112 bp) when the cytosines at the fourth and fifth CpG dinucleotides (indicated with orange rectangle) are methylated. Both methylated (M)- and unmethylated (U)-specific bands are identified in the chorionic villus sample. V, villi; L, leukocytes; and N.C, negative control.

the deleted region of the first child and the mother, delineating two signals on villus cell interphase spreads (Fig. 1). Next combined bisulfite restriction analysis (COBRA) was performed for the IG-DMR and the *MEG3*-DMR using villus cell genomic DNA, identifying both methylated- and unmethylated allele-specific bands (Fig. 1B). These findings clearly excluded the presence of a microdeletion in the fetus by 14 weeks of gestation. Subsequent pregnant course was uneventful, and a phenotypically normal infant was delivered at term by a caesarean section.

To our knowledge, this is the first report describing a prenatal genetic testing for a familial microdeletion affecting the chromosome 14q32.2 imprinted region. Although such a genetic testing is possible only when an accurate genetic diagnosis has been made for the proband, it permitted the precise diagnosis before the second to the third trimester when characteristic UPD(14)pat-like features such as bell-shaped small thorax with coat hanger appearance and polyhydroamnios become detectable by ultrasonographic studies [Suzumori et al., 2010; Yamanaka et al., 2010]. Such an early prenatal diagnosis, though it is associated with a certain risk such as CVS-induced abortion, provides critical information for the clinical management. When a microdeletion is excluded as shown in this case, this releases the parents from the anxiety of having an affected fetus and allows for a standard follow-up during pregnancy. By contrast, when a microdeletion is identified, this will allow for appropriate management during pregnancy (e.g., amnioreduction to mitigate the risk of threatened premature delivery) and pertinent therapeutic interventions for the infant (e.g., respiratory management). Thus, prenatal genetic diagnosis appears to be beneficial for the fetus and the parents, when it is performed at appropriate institutes where a multidisciplinary team including a genetic counselor is available.

ACKNOWLEDGMENTS

This work was supported by Grants-in-Aid for Scientific Research (A) (22249010 and 25253023) and Research (B) (21028026) from the Japan Society for the Promotion of Science, by Grants for Research on Intractable Diseases (H22-161) from the Ministry of Health, Labor and Welfare (MHLW), by Grants for National Center for Child Health and Development (23A-1, 25-10), and by Grants from Takeda Science Foundation, Novartis Foundation, and The Japan and Foundation for Pediatric Research.

REFERENCES

da Rocha ST, Edwards CA, Ito M, Ogata T, Ferguson-Smith AC. 2008. Genomic imprinting at the mammalian Dlk1-Dio3 domain. Trends Genet 24:306–316.

Kagami M, Nishimura G, Okuyama T, Hayashidani M, Takeuchi T, Tanaka S, Ishino F, Kurosawa K, Ogata T. 2005. Segmental and full paternal isodisomy for chromosome 14 in three patients: Narrowing the critical region and implication for the clinical features. Am J Med Genet Part A 138A:127–132.

Kagami M, Sekita Y, Nishimura G, Irie M, Kato F, Okada M, Yamamori S, Kishimoto H, Nakayama M, Tanaka Y, Matsuoka K, Takahashi T, Noguchi M, Tanaka Y, Masumoto K, Utsunomiya T, Kouzan H, Komatsu Y, Ohashi H, Kurosawa K, Kosaki K, Ferguson-Smith AC,

Ogata T. 2008a. Deletions and epimutations affecting the human 14q32.2 imprinted region in individuals with paternal and maternal upd(14)-like phenotypes. Nat Genet 40:237–242.

Kagami M, Yamazawa K, Matsubara K, Matsuo N, Ogata T. 2008b. Placentomegaly in paternal uniparental disomy for human chromosome 14. Placenta 29:760–761.

Kagami M, O'Sullivan MJ, Green AJ, Watabe Y, Arisaka O, Masawa N, Matsuoka K, Fukami M, Matsubara K, Kato F, Ferguson-Smith AC, Ogata T. 2010. The IG-DMR and the MEG3-DMR at human chromosome 14q32.2: Hierarchical interaction and distinct functional properties as imprinting control centers. PLoS Genet 6:e1000992.

Kagami M, Kato F, Matsubara K, Sato T, Nishimura G, Ogata T. 2012. Relative frequency of underlying genetic causes for the development of UPD(14)pat-like phenotype. Eur J Hum Genet 20:928–932.

Suzumori N, Ogata T, Mizutani E, Hattori Y, Matsubara K, Kagami M, Sugiura-Ogasawara M. 2010. Prenatal findings of paternal uniparental disomy 14: Delineation of further patient. Am J Med Genet Part A 152A:3189–3192.

Yamanaka M, Ishikawa H, Saito K, Maruyama Y, Ozawa K, Shibasaki J, Nishimura G, Kurosawa K. 2010. Prenatal findings of paternal uniparental disomy 14: Report of four patients. Am J Med Genet Part A 152A:789–791.

RESEARCH LETTER

AMERICAN JOURNAL OF medical genetics PART A

Mosaic upd(7)mat in a Patient With Silver–Russell Syndrome

Tomoko Fuke-Sato,[1,2] Kazuki Yamazawa,[1] Kazuhiko Nakabayashi,[3] Keiko Matsubara,[1] Kentaro Matsuoka,[4] Tomonobu Hasegawa,[2] Kazushige Dobashi,[5] and Tsutomu Ogata[1,6]*

[1]Department of Molecular Endocrinology, National Research Institute for Child Health and Development, Tokyo, Japan

[2]Department of Pediatrics, Keio University School of Medicine, Tokyo, Japan

[3]Department of Maternal-Fetal Biology, National Research Institute for Child Health and Development, Tokyo, Japan

[4]Division of Pathology, National Medical Center for Children and Mothers, Tokyo, Japan

[5]Department of Pediatrics, Showa University School of Medicine, Tokyo, Japan

[6]Department of Pediatrics, Hamamatsu University School of Medicine, Hamamatsu, Japan

Received 10 March 2011; Accepted 9 November 2011

TO THE EDITOR:

Silver–Russell syndrome (SRS) is a congenital developmental disorder characterized by pre- and post-natal growth failure, relative macrocephaly, triangular face, hemihypotrophy, and 5th finger clinodactyly [Russell, 1954; Silver et al., 1953]. Recent studies have shown that hypomethylation (epimutation) of the paternally derived differentially methylated region (DMR) in the upstream of *H19* (*H19*-DMR) on chromosome 11p15 and maternal uniparental disomy for chromosome 7 (upd(7)mat) account for ~45% and ~5–10% of SRS patients, respectively [Eggermann, 2010; Binder et al., 2011]. Furthermore, consistent with the involvement of imprinted genes in both body and placental growth [for review, Coan et al., 2005], epimutations of the *H19*-DMR and upd(7)mat are known to result in placental hypoplasia [Yamazawa et al., 2008a,b]. Here, we report on a Japanese boy with mosaic upd(7)mat who was identified through genetic screenings in 120 patients with SRS-like phenotype.

This Japanese boy was conceived naturally to a 41-year-old father and a 36-year-old mother. The parents were non-consanguineous and healthy. The paternal height was 165 cm (−0.9 SD), and the maternal height 155 cm (−0.6 SD).

At 35 weeks of gestation, he was delivered by a cesarean because of fetal distress. At birth, his length was 37.4 cm (−3.1 SD), his weight 1.28 kg (−3.1 SD), and his head circumference 29.0 cm (−1.3 SD). The placenta weighed 400 g (−0.6 SD [Kagami et al., 2008]). Shortly after birth, he was found to have ventricular septal defect, hydronephrosis, and abnormal external genitalia (hypospadias, bifid scrotum, and bilateral cryptorchidism). He received orchidopexy at $1^{10}/_{12}$ years of age and genitoplasty at $2^{4}/_{12}$ years of age. He exhibited feeding difficulty and speech delay.

At $5^{1}/_{12}$ years of age, he was referred because of short stature. His height was 87.9 cm (−4.3 SD), weight was 10.4 kg (−2.9 SD), and his head circumference 49.0 cm (−0.7 SD). Physical examination showed relative macrocephaly, abnormal teeth, 5th finger clinodactyly, and underdeveloped muscles. There was no hemihypotrophy. Endocrine studies for short stature yielded normal results, as did radiological examinations. His karyotype was 46,XY in all the 50 lymphocytes examined. He was clinically diagnosed as having SRS, and molecular studies were performed after obtaining the approval from the Institutional Review Board Committee at National Center for Child Health and Development and the written informed consent from the parents.

We first performed methylation analysis of the *MEST*-DMR on chromosome 7q32.2 using leukocyte genomic DNA by the previously described methods [Yamazawa et al., 2008b], because this patient showed relatively mild SRS-phenotype with speech delay

How to Cite this Article:
Fuke-Sato T, Yamazawa K, Nakabayashi K, Matsubara K, Matsuoka K, Hasegawa T, Dobashi K, Ogata T. 2012. Mosaic upd(7)mat in a patient with Silver–Russell syndrome.
Am J Med Genet Part A 158A:465–468.

Grant sponsor: Japan Society for the Promotion of Science (JSPS); Grant number: 22249010; Grant sponsor: Ministry of Health, Labor and Welfare; Grant number: H21-005; Grant sponsor: Grant of National Center for Child Health and Development; Grant number: 23A-1.

*Correspondence to:
Tsutomu Ogata, M.D., Department of Pediatrics, Hamamatsu University School of Medicine, Hamamatsu 431-3192, Japan.
E-mail: tomogata@hama-med.ac.jp

Published online 13 January 2012 in Wiley Online Library (wileyonlinelibrary.com).
DOI 10.1002/ajmg.a.34404

and feeding difficulty characteristic of upd(7)mat [Hitchins et al., 2001; Kotzot, 2008]. The methylation analysis showed a major peak for methylated clones and a minor peak for unmethylated clones in this patient (Fig. 1A). We also examined the *H19*-DMR and other multiple DMRs on various chromosomes by the bio-COBRA (combined bisulfite restriction analysis) method, as reported previously [Yamazawa et al., 2010]. The *GRB10*-DMR on chromosome 7p12.1 and the *PEG10*-DMR on chromosome 7q21.3 exhibited skewed methylation patterns consistent with the predominance of maternally derived clones, as did the *MEST*-DMR (Fig. 1B). By

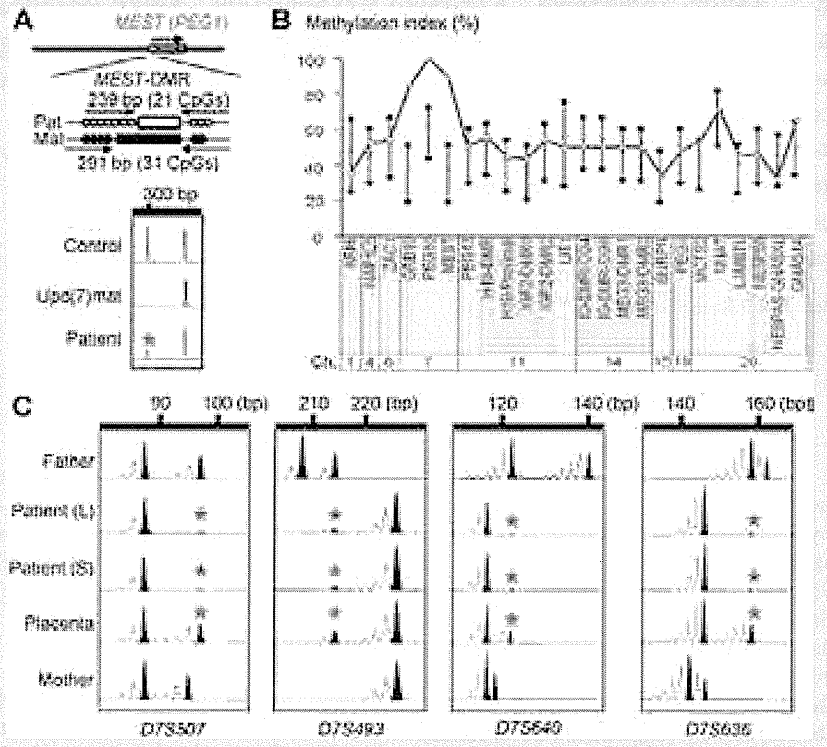

FIG. 1. Representative molecular results. A: Methylation analysis for the *MEST*-DMR. The methylated and unmethylated allele-specific primers were designed to yield PCR products of different sizes, and the PCR products were visualized on the 2100 Bioanalyzer (Agilent, Santa Clara, CA). Both methylated and unmethylated alleles are amplified in a control subject, and the methylated allele only is identified in a previously reported patient with upd(7)mat [Yamazawa et al., 2008b]. In this patient, a major peak for the methylated allele and a minor peak for the unmethylated allele (a red asterisk) are delineated. B: Methylation indices of 24 DMRs examined by the bio-COBRA. The PCR products were digested with methylation sensitive restriction enzymes, and the methylation indices (the ratios of methylated clones) were calculated using peak heights of digested and undigested fragments on the 2100 Bioanalyzer using 2100 expert software. The black vertical bars indicate the reference data in 20 normal control subjects (maximum – minimum). The DMRs highlighted in blue and pink are methylated after paternal and maternal transmissions, respectively.
C: Microsatellite analysis. Major peaks of maternal origin and minor peaks of paternal origin (red asterisks) are identified in this patient. The minor peaks of paternal origin are more obvious in the placenta than in the leukocytes (L) and salivary cells (S). Calculation of the mosaic ratio using the *D7S507* data, under the assumption of no trisomic cells. For this locus, the patient is considered to be heterozygous with the major 87 bp peak of maternal origin and a minor 97 bp peak of paternal origin. The father is also heterozygous with the two peaks of the same sizes, and the area under curve (AUC) is larger for the short 87 bp peak than for the long 97 bp peak. This unequal amplification is consistent with short products being more easily amplified than long products. In this patient, the AUC ratio between the major 87 bp peak and the minor 97 bp peak is obtained as 1.0:0.043 for leukocytes, 1.0:0.044 for salivary cells, and 1.0:0.803 in placental tissue, after compensation of the unequal amplification between the two peaks using the paternal data. Here, let "XL" represent the frequency of the upid(7)mat cells in leukocytes (thus, (1 – XL) denotes the frequency of normal cells in leukocytes). Then, the paternally derived 97 bp peak is generated by one paternally derived chromosome in the normal cells, that is, (1 – XL), and the maternally derived 87 bp peak is formed by the products from two maternally derived homologous chromosomes in the upid(7)mat cells and one maternally derived chromosome in the normal cells, that is, $\{2XL + (1 - XL)\} = (XL + 1)$. Thus, the AUC ratio between the two peaks is represented as $(XL + 1):(1 - XL) = 1.0:0.043$, and "XL" is calculated as 0.92 (92%). Similarly, when "XS" and "XP" represent the frequency of the upid(7)mat cells in salivary cells and placental tissue, respectively, "XS" is obtained as 0.91 (91%) and "XP" as 0.11 (11%). Furthermore, when "XB" represents the frequency of the upid(7)mat cells in buccal epithelium cells, "XB" is obtained as 0.91 (91%), on the basis of the previous report that salivary cells comprises ~40% of buccal epithelium cells and ~60% of leukocytes [Thiede et al., 2000].

TABLE I. The Results of Microsatellite Analysis

Locus	Position	Father	Patient (L)	Patient (S)	Placenta	Mother	Assessment
D7S517	7p22.2	254/258	(254)/258	(254)/258	(254)/258	256/258	Maternal Iso-D[a]/biparental
D7S507	7p15–21	87/97	87/(97)	87/(97)	87/(97)	87/95	Maternal Iso-D[a]/biparental
D7S493	7p15.3	208/214	(214)/226	(214)/226	(214)/226	226	Maternal D[b]/biparental
D7S484	7p14–15	96/100	(96)/98	(96)/98	(96)/98	98/100	Maternal Iso-D/biparental
D7S502	7q11.12	298	294/(298)	294/(298)	294/(298)	294/304	Maternal Iso-D/biparental
D7S669	7q11.2	116/126	(116)/124	(116)/124	(116)/124	124	Maternal D[b]/biparental
D7S515	7q21–22	169/173	171/(173)	171/(173)	171/(173)	169/171	Maternal Iso-D/biparental
D7S640	7q21.1–31.2	122/140	116/(122)	116/(122)	116/(122)	116/118	Maternal Iso-D/biparental
D7S684	7q34	169/179	177/(179)	177/(179)	177/(179)	177/179	Not informative
D7S636	7q35–36	158/162	146/(158)	146/(158)	146/(158)	142/146	Maternal Iso-D/biparental
D7S798	7q36	73/79	(79)/83	(79)/83	(79)/83	73/83	Maternal Iso-D/biparental

L, leukocytes; S, salivary cells; D, disomy.
The Arabic numbers denote the PCR product sizes in bp.
The minor peaks are indicated in parentheses.
[a]On the basis of the results of other informative loci, the major peaks are considered to be of maternal origin.
[b]Because of the maternal homozygosity, disomic status (isodisomy or heterodisomy) is unknown for these loci.

contrast, other DMRs including the *H19*-DMR showed normal methylation patterns.

We next performed microsatellite analysis for 11 loci on various parts of chromosome 7, using genomic DNA from leukocytes of the patient and the parents, from salivary cells of the patient, and from formalin-fixed and paraffin-embedded placental tissue. Major peaks consistent with maternal uniparental isodisomy and minor peaks of paternal origin were unequivocally identified for *D7S484*, *D7S502*, *D7S515*, *D7S640*, *D7S636*, and *D7S798*; furthermore, similar patterns were also detected for *D7S517*, *D7S507*, *D7S669*, and *D7S493*, although the results were not informative for *D7S684* (Fig. 1C and Table I). The minor peaks of paternal origin were similar between leukocytes and salivary cells and more evident in placental tissue. These findings, together with the normal karyotype in lymphocytes, indicated mosaic full maternal isodisomy for chromosome 7 (upid(7)mat) in this patient. Furthermore, since such a condition is frequently associated with mosaicism for trisomy 7 [Petit et al., 2011], we performed fluorescence in situ hybridization (FISH) analysis for stocked lymphocyte pellets, using a CEP7 probe for *D7Z1* (Abbott Laboratories, Abbott Park, IL). The FISH analysis identified two normal signals in 995 of 1,000 interphase nuclei examined, with no trace of trisomic nuclei; while a single signal was delineated in the remaining five nuclei, this was regarded as a false-positive finding. Thus, assuming no trisomic cells, the frequency of the full upid(7)mat cells was calculated as 92% in leukocytes, using the results of *D7S507* (Fig. 1C). In addition, similarly assuming no trisomic cells in other tissues, the frequency of the full upid(7)mat cells was calculated as 91% salivary cells (and in buccal cells) and 11% in placental tissue, although we could not perform FISH analysis in buccal cells and placental cells.

These results imply that this patient had an abnormal cell lineage with full upid(7)mat and a normal cell lineage with biparentally inherited chromosome 7 homologs at least in lymphocytes, and these had no trisomy 7. It is likely that mitotic non-disjunction and subsequent trisomy rescue (loss of the paternally derived chromosome 7 from a trisomic cell) took place in the post-zygotic developmental stage, resulting in the production of the mosaic full upid(7)mat (Fig. 2). While full upid(7)mat can also be produced by monosomy rescue (duplication of a single maternally derived chromosome 7 in a zygote), this mechanism is predicted to cause non-mosaic rather than mosaic upid(7)mat [Miozzo et al., 2001]. Although it remains to be clarified why trisomic cells mediating the production of full upid(7)mat cells were apparently absent in lymphocytes of this patient, there might be a negative selection against lymphocytes with trisomy 7.

However, the presence or absence of demonstrable trisomic cells was studied only in lymphocytes. In this regard, trisomic cells have been identified more frequently in skin fibroblasts and amniocytes than in blood cells in patients with mosaic trisomy 7 [Chen et al., 2010; Petit et al., 2011], and they are usually more frequently detected in the placental tissue than in the body tissue, as has been demonstrated by confined placental trisomy [Kalousek et al., 1991]. These findings would argue for the possible presence of trisomic cells in several tissues including placenta of this patient.

The full upid(7)mat cells were assessed to account for the majority of the leukocytes and salivary cells (buccal cells) and the minority of the placental tissue, under the assumption of no

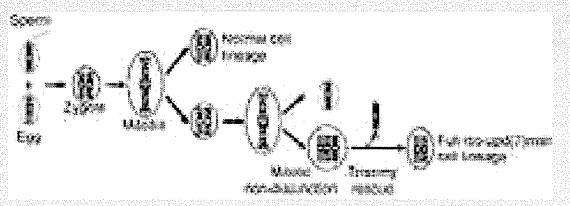

FIG. 2. Schematic representation of the generation of the mosaic upid(7)mat. The maternally and paternally derived chromosome 7 homologs are shown in red and blue, respectively. In this figure, mitotic non-disjunction is assumed at the second mitosis.